Received: 17 April 2021 | Accepted: 7 June 2021

DOI: 10.1002/ame2.12178

ORIGINAL ARTICLE

A novel rat tail disc degeneration model induced by static bending and compression

Yichao Ji | Pengfei Zhu | Linlin Zhang | Huilin Yang

Department of Orthopaedic Surgery, The First Affiliated Hospital of Soochow University, Suzhou, P.R. China

Correspondence
Linlin Zhang and Huilin Yang, Department of Orthopaedic Surgery, The First Affiliated Hospital of Soochow University, 188 Shizi St., Suzhou, Jiangsu 215006, China.
Email: zhangdoublelin@139.com (L. Z.) and hlyang@suda.edu.cn (H. Y.)

Abstract

Background: A new rat tail intervertebral disc degeneration model was established to observe the morphologic and biologic changes of static bending and compression applied to the discs.

Methods: In total, 20 Sprague-Dawley rats with similar weight were randomly divided into 4 groups. Group 1 served as a control group for a baseline assessment of normal discs. Group 2 underwent a sham surgery, using an external device to bend the vertebrae of coccygeal 8-10. Groups 3 and 4 were the loaded groups, and external devices were instrumented to bend the spine with a compression level of 1.8 N and 4.5 N, respectively. Magnetic resonance imaging (MRI), histological, and quantitative real-time PCR (qRT-PCR) analysis were performed on all animals on day 14 of the experiment.

Results: Magnetic resonance imaging and histological results showed that the changes of intervertebral disc degeneration increased with the size of compression load. Some architecture disorganizations in nucleus pulposus and annulus fibrosus were found on both of the convex and concave side in the groups of 1.8 N and 4.5 N. An upregulation of MM-3, MM-13, and collagen 1-α1 mRNA expression and a downregulation of collagen 2-α1 and aggrecan mRNA expression were observed in the sham and loading groups. Significant changes were found between the loading groups, whereas the sham group showed similar results to the control group.

Conclusions: Static bending and compression could induce progressive disc degeneration, which could be used for biologic study on disc degeneration promoted by static complex loading.

KEYWORDS

animal model, annulus fibrosus, bending and compression, disc degeneration, nucleus pulposus

1 | INTRODUCTION

Low back pain (LBP) is one of the most common public health problems in many countries today, placing a heavy burden on national health care systems and economies. Despite the high incidence of LBP, the pathophysiology and pathogenesis of LBP are still poorly understood. Intervertebral disc degeneration (IDD) is generally considered to be the most critical and closely associated disease with LBP, characterized by cellular dysfunction and loss of proteoglycan production.[1-3] IDD is caused by many factors, among which mechanical factors play an important role. Persistent abnormal postures such as bending, twisting, sitting, and lifting objects are thought to cause disc degeneration.

The human intervertebral disc is subjected to a constant and complex load. This load comes from a combination of weight, muscle, and ligament tension.[4] It seems that a disc is most likely to sustain mechanical damage when loaded in a flexed posture.[5] To counteract the flexion torque caused by weight, the muscles at the back of the spine must exert a force, which causes the discs to be subjected to high pressure.[6] Disc bulges or protrusions often pre-exist in patients with acute back pain, which suggests that repeated compressive loads may gradually result in a herniated intervertebral disc.[7] However, this hypothesis has not yet been tested in animal models.

The aim of this study is to establish an animal model that can simulate the complex mechanical load of human intervertebral disc during bending. We tested the hypothesis that a disc herniation could be gradually induced by static complex loading.

2 | MATERIALS AND METHODS

2.1 | Experimental animals

Approval was obtained from the ethics committee of Soochow University. Twenty 12-week-old male Sprague-Dawley rats were selected in this study. The 20 rats were randomly divided into 4 groups. Group 1, a control group, was assessed for normal discs as a baseline (n = 5). Other rats had an external device implanted in the coccygeal 8-10 vertebrae to bend the spine at a fixed angle. Rats in group 2 underwent a sham surgery with no load (n = 5). In groups 3 and 4, rats were subjected to compression load of 1.8 N and 4.5 N, respectively.

2.2 | Surgical procedure

Rats in groups 2-4 were anesthetized by intraperitoneal injection of 1% pentobarbital sodium (40 mg/kg). The tail of the rats was cleaned and disinfected with 70% ethanol solution. The Co8-10 intervertebral disc space was positioned by hand, and the corresponding skin area was marked. Using an electric drill and 2 K-wires (length 50 mm; diameter 1.2 mm), the vertical body was inserted percutaneously near the labeled disc, so that it was placed vertically in the center of the Co8 and Co10 vertebral bodies. Alignment jigs were used to assist in the precise positioning and arrangement of the wires (Figure 1A). The 2 wires were fixed on the concave side of the curved tail at an angle of 40° (Figure 1B). The tension springs were placed on the convex side between the 2 wires, 25 mm from the center of the shaft of the tail. Plastic plates were used to prevent the tail from twisting (Figure 1C).

2.3 | Magnetic resonance imaging (MRI)

At 14 days postoperatively, MRI was performed on all experimental rats using the 1.5 Tesla system (General Electric Company, Chicago, USA). The imaging sequence consisted of coronal spin echo T2-weighted images (repletion time 3000 ms; echo time 80 ms; field of view 200 × 200 mm; slice thickness 1.4 mm). Four blinded investigators used the Pfirrmann classification to classify disc images into 5 grades.[8]

2.4 | Histological analysis

After the MRI examination was completed, the animals were euthanized with a lethal dose of anesthetic. The target Co8-10 vertebral body was removed, the skin and soft tissue were separated, and the Co8-Co9 and Co9-Co10 intervertebral discs were removed. Co9-Co10 intervertebral discs were collected and flash frozen in liquid nitrogen. The remaining tissues were fixed in 10% buffer formaldehyde solution for 24 hours and decalcified in 10% ethylenediaminetetraacetic acid (EDTA) for 30 days. After paraffin embedding, the tissues were prepared into paraffin sections with a thickness of 5 μm. Histological scores were determined using hematoxylin/eosin, safranin O/Fast green, and Mallory staining. Images were obtained using an Axio Imager (Carl Zeiss, Jena, Germany). Histological score was determined according to the histological characteristics of the nucleus pulposus and annulus fibrosus. Four blinded investigators used the Norcross classification to evaluate sections ranging from 10 for no degeneration to 2 for severe degeneration.[9]

2.5 | Gene expression

Disc (Co9-Co10) was dissected and prepared for a gene expression test as described previously.[10] The nucleus pulposus tissues were ground and crushed, and total RNA was extracted with Trizol reagent and purified with RNeasy Mini Kit (Qiagen, Hilden, Germany). Reverse transcription of mRNA was performed using the RevertAid First Strand cDNA Synthesis Kit (Thermo, Vilnius, Lithuania). To determine the quantitative expression of mRNA, the iTaq Universal SYBR Green Supermix Kit was used to amplified cDNA equivalent to 20 μg total RNA (Bio-Rad, Hercules, CA, USA) on a CFX96 Real-Time PCR System (Bio-Rad), following the manufacturer's protocol. The expression of 3 anabolic genes (collagen 1-α1, collagen 2-α1 and

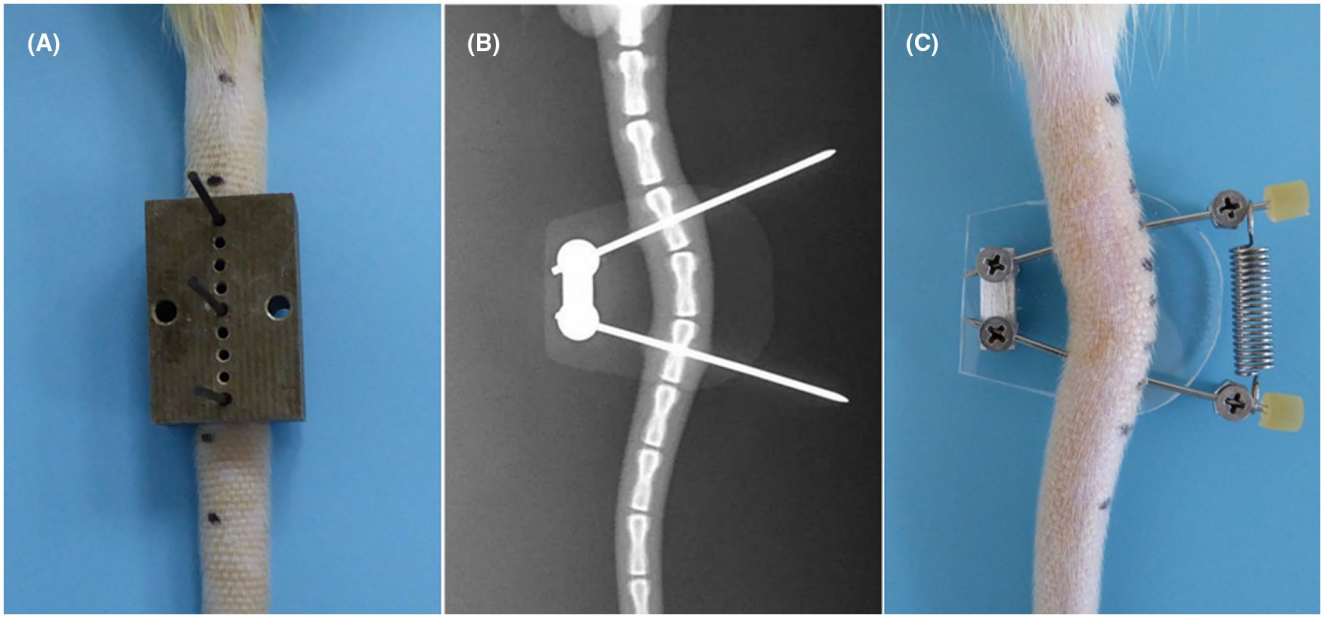

FIGURE 1 A, An alignment jig for a precise location of the wires. B, Two wires were fixed at a 40° angle. C, Tension springs were placed between the 2 wires on the convex side. A plastic plate was used to prevent vertebrae torsion

TABLE 1 Primers used for quantitative real-time PCR

Gene	Forward Primer sequence (5′-3′)	Reverse Primer sequence (5′-3′)
GAPDH	CAAGTTCAACGGCACAGTCAAG	ACATACTCAGCACCAGCATCAC
Collagen1-α1	GCCCAGAAGAATATGTATCACCAGA	GGCCAACAGGTCCCCTTG
Collagen2-α1	ATGAGGGCCGAGGGCAACAG	GATGTCCATGGGTGCAATGTCAA
Aggrecan	TCCGCTGGTCTGATGGACAC	CCAGATCATCACTACGCAGTCCTC
MMP-3	TGGACCAGGGACCAATGGA	GGCCAAGTTCATGAGCAGCA
MMP-13	CCCTGGAGCCCTGATGTTT	CTCTGGTGTTTTGGGGTGCT

aggrecan) and 2 catabolic genes (MMP-3 and MMP-13) was analyzed. Glyceraldehyde-3-phosphate dehydrogenase (GAPDH) was used as the internal standard. The relative transcription levels were calculated by the $2^{-\Delta\Delta ct}$ method and normalized to the expression of the reference gene GAPDH. The specific primer sequences are presented in Table 1.

2.6 | Statistical analysis

All experimental data were expressed as mean ± SD. Software Statview (SAS Institute, Cary, NC, USA) was used for statistical analysis; $P < .05$ indicates a significant difference. Analysis of variance (ANOVA) with Fisher's protected least significant difference (PLSD) was used to determine significant differences between groups in MRI and histomorphological grading assessments. For qRT-PCR data, Fisher's PLSD with a hypothesized mean of 1 was first used to test the difference between the experimental groups (groups 2-4) and the control group (group 1). Next, an ANOVA with Fisher's PLSD was performed to assess whether there were differences between the experimental groups.

3 | RESULTS

3.1 | MRI assessment of degeneration

Figure 2 shows the T2-weighted image of the target coccygeal disc of the rats taken 14 days after the experiment. The scores of intervertebral disc degeneration were significantly higher in the loaded groups than in the sham group ($P < .05$). The 2 loading groups had a significant difference in disc degeneration ($P < .05$). However, there was no statistically significant difference in MRI evaluations between the sham and the control groups ($P > .05$) (Figure 3A).

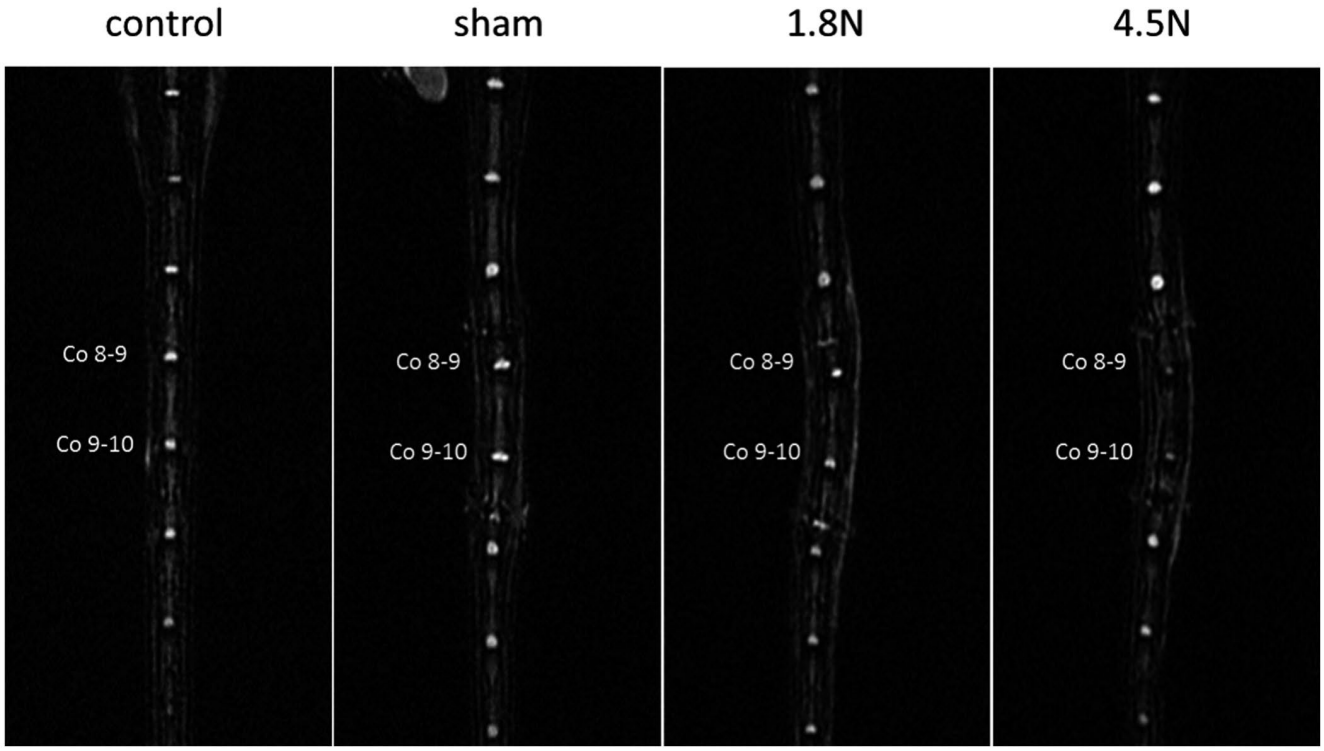

FIGURE 2 Representative T2-weighted sagittal MRIs in different groups, 14 d after the experiment

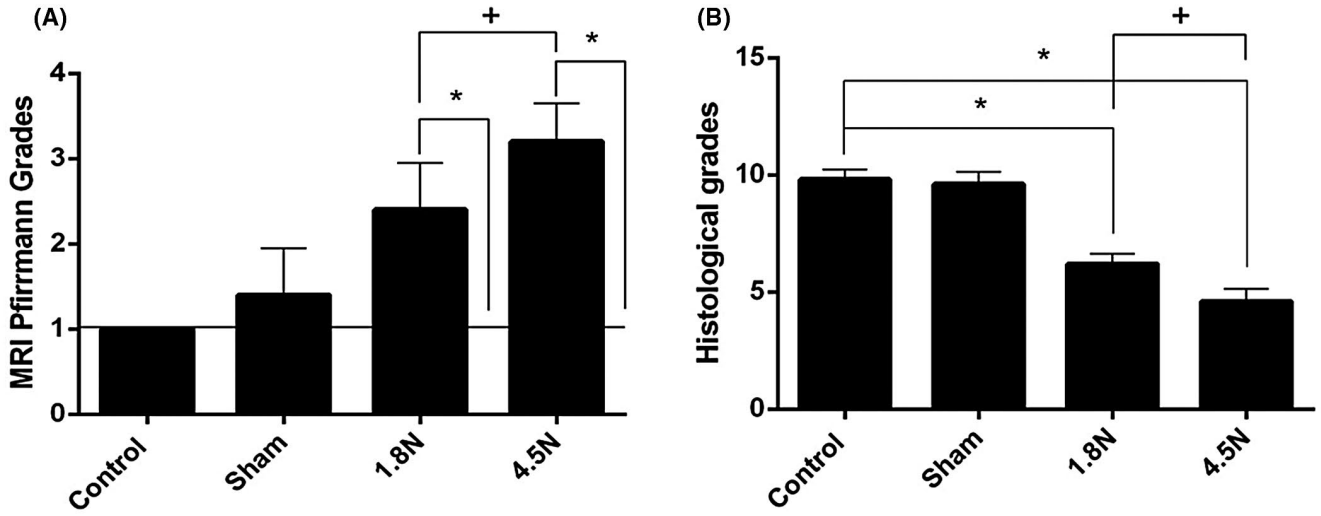

FIGURE 3 A, Changes in the MRI Pfirrmann classification score. B, Changes in the histology Norcross score; $^{*,+}P < .05$

3.2 | Histological evaluation

Different groups of histological sections showed different morphological changes in the nucleus pulposus and annulus fibrosus. Annular protrusion and nucleus pulposus migration were histologically observed in the loading groups (Figure 4). The histological scores for the 1.8-N and 4.5-N groups were significantly lower than those in the unloaded groups and decreased gradually with the degree of compression ($P < .05$). The results of the sham group were similar to those of the normal group ($P > .05$) (Figure 3B).

3.3 | Gene expression

Aggrecan and collagen 2-α1 were significantly downregulated, whereas collagen 1-α1, MMP-1, and MMP-13 were upregulated with significant differences between the loading groups and the control

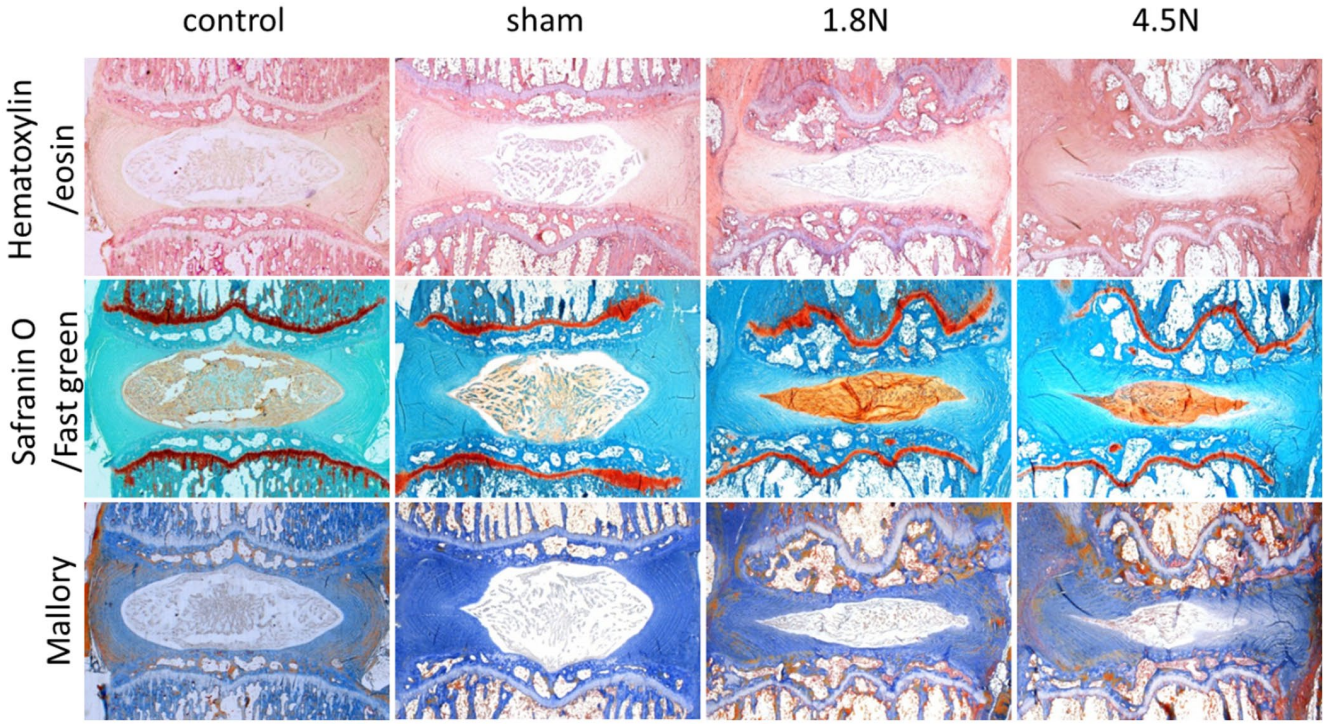

FIGURE 4 Representative hematoxylin/eosin, safranin O/Fast green, and Mallory staining images of the whole experimental disc (original magnification ×25)

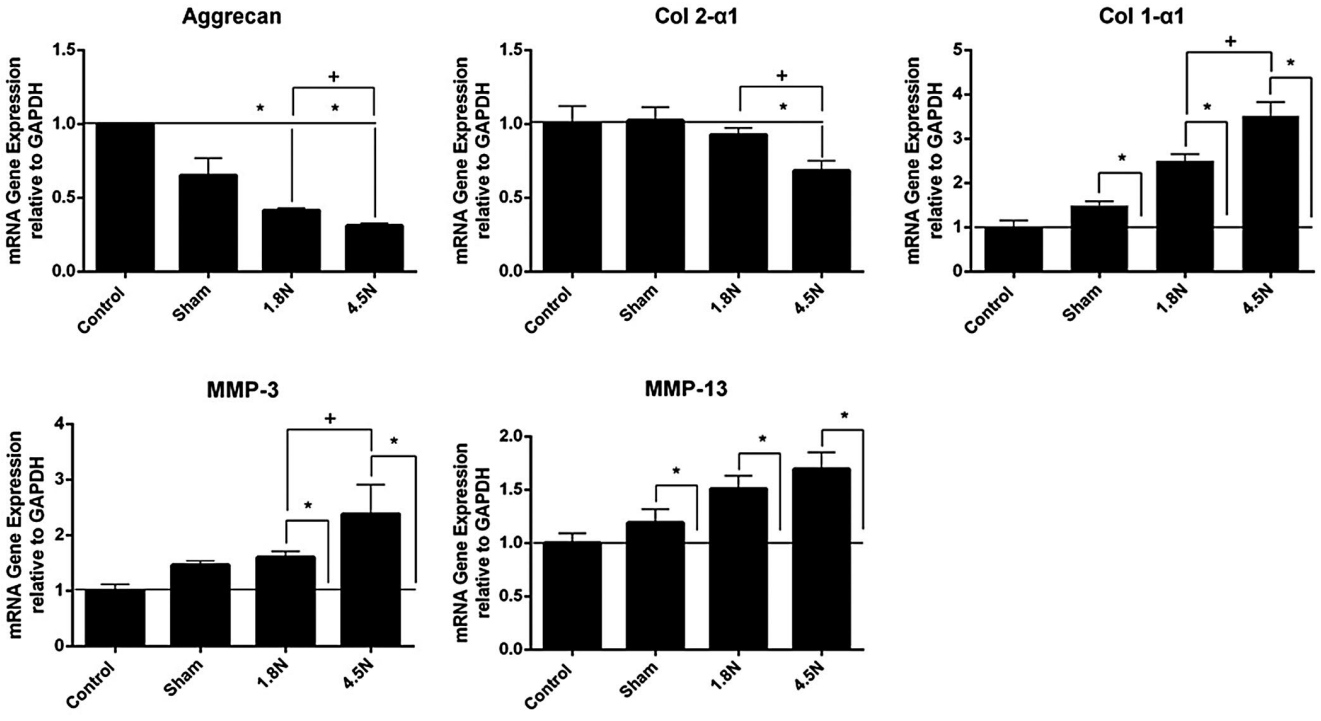

FIGURE 5 Real-time PCR gene expression profile in the control, sham, 1.8-N, and 4.5-N groups. The mRNA levels of aggrecan, collagen 2-α1, collagen 1-α1, MMP-3, and MMP-13 normalized to GAPDH are shown in the experimental groups relatively to the control disc, $^{*,+}P < .05$

group. However, the sham group showed results similar to the control group except for the collagen 1-α1 expression. All tested genes but MMP-13 exhibited a significant change when comparing the 1.8-N group with the 4.5-N group (Figure 5).

4 | DISCUSSION

We established an in vivo model of the rat tail in which different compressive loads were applied to a bent intervertebral disc. The most striking thing we found in this study was that static complex loading can induce posterior intervertebral disc protrusion when combining bending and compression loads but not during bending alone. We compared the morphological and biological changes occurring in the intervertebral disc under different static complex loads.

In general, disc herniation is caused by disc degeneration and is characterized by disc dehydration. Disc dehydration results from a decrease in proteoglycan content that is normally involved in binding water with negative charge.[11] MRI showed disc degeneration with loss of intranuclear T2 hyperintensity. The observed MRI grades of disc degeneration increased with the magnitude of compressive load. The intervertebral discs in the control group and the sham group showed uniform structure and bright high-intensity white signal. Disc bulge could be seen in the compressive loading groups. In the 1.8-N group, the disc structure was not homogeneous and showed high-intensity white signal. In contrast, the disc structure of the 4.5-N group was inhomogeneous as well, but the signal was of moderate gray intensity.

The histomorphological grades decreased with the magnitude of the compressive loads. When comparing discs between the control, the 1.8-N, and the 4.5-N groups, it could be observed that the histological scores decreased in parallel with the compression. On the convex side, there was some disorganization and protrusion in the lamellar architecture of the annulus, for the 1.8-N and 4.5-N groups. An upregulation of catabolic mRNA expression (MM-3 and MM-13) and a downregulation of anabolic mRNA expression (collagen 2-α1 and aggrecan) were observed in all experimental groups. Degenerative nucleus pulposus was replaced by fibrous tissue, which may account for the increase in collagen 1-α1 expression in the loading groups. These results are consistent with previous findings reporting that static compressive stress would induce intervertebral disc degeneration.[12,13] Various rat tail compression models have been established in previous studies.[14-17] Iatridis et al[14] initially used an Ilizarov-type instrument to describe the rat tail compression model for the application of chronic compression. Ching et al[15] studied the differences between static loading and cyclical loading on the rat-tail intervertebral disc. The researchers noted that the disc height decreased significantly in the static compression group. Lotz et al[17] analyzed how static compression loads affect the biomechanics of the tail intervertebral disc. They found that compressive loading resulted in progressive annulus disorganization, which is a dose-dependent apoptotic response with downregulated expression of collagen 2 and aggrecan genes. Court et al[16] were the first to study the role of static bending in the morphology and biology of the murine intervertebral disc. Compression consisted of a load applied on the concave side of the bent rat tail by a calibrated elastic band. With this model, they concluded that excessive matrix compression affected annular cell death, but the gene expression of collagen 2 was negatively regulated by the static nature of the load. However, all the above studies did not examine the interaction of biology and structure that was associated with static complex loading; this may be one of the important factors that lead to disc herniation.

The limitation of this study is that, although the rodent tail discs are biomechanically and compositionally similar to human lumbar discs, there are significant differences. Tail intervertebral discs in rats are less burdened and have different anatomical structures and specific sizes. Moreover, there are differences in cell biology and biochemistry between the nucleus pulposus in rats and mature humans. The relatively small number of animals in each group, just 5, increases the likelihood of type II error. This rat-tail model truly simulates the human disc loading in a flexion posture, though the limitations above exist. Consequently, this model reliably provides relevant relationship between disc herniation and static complex loading.

In conclusion, static complex loading can induce posterior intervertebral disc protrusion when combining bending and compression loads but not during bending alone. This model can be used to evaluate the mechanobiological changes associated with disc herniation under complex loads.

CONFLICT OF INTEREST

YJ, PZ, LZ, and HY have no conflicts of interest relevant to this article.

AUTHOR CONTRIBUTIONS

HY contributed to the study conception and design. Data collection and analysis were performed by YJ and PZ The first draft of the manuscript was written by YJ LZ revised the manuscript critically for important intellectual content. All authors commented on previous versions of the manuscript. All authors read and approved the final manuscript.

ETHICS APPROVAL

Approval was obtained from the ethics committee of Soochow University.

CONSENT TO PARTICIPATE

Not applicable.

CONSENT FOR PUBLICATION

Not applicable.

DATA AVAILABILITY STATEMENT

Not applicable.

ORCID

Linlin Zhang https://orcid.org/0000-0002-9139-2315

REFERENCES

1. Zheng CJ, Chen J. Disc degeneration implies low back pain. *Theor Biol Med Modell*. 2015;12:24.
2. Weber KT, Jacobsen TD, Maidhof R, et al. Developments in intervertebral disc disease research: pathophysiology, mechanobiology, and therapeutics. *Curr Rev Musculoskeletal Med*. 2015;8:18-31.
3. Luoma K, Riihimäki H, Luukkonen R, Raininko R, Viikari-Juntura E, Lamminen A. Low back pain in relation to lumbar disc degeneration. *Spine*. 2000;25:487-492.
4. Mietsch A, Kletsas D, Pratsinis H, et al. Mechanical loading of the intervertebral disc: from the macroscopic to the cellular level. *Eur Spine J*. 2014;23:333-343.
5. Veres SP, Robertson PA, Broom ND. Issls prize winner: how loading rate influences disc failure mechanics a microstructural assessment of internal disruption. *Spine*. 2010;35:1897-1908.
6. Han KS, Rohlmann A, Yang SJ, Kim BS, Lim TH. Spinal muscles can create compressive follower loads in the lumbar spine in a neutral standing posture. *Med Eng Phys*. 2011;33:472-478.
7. Shymon SJ, Burt Y, Dwek JR, Proudfoot JA, Michael D, Hargens AR. Altered disc compression in children with idiopathic low back pain: an upright magnetic resonance imaging backpack study. *Spine*. 2014;39:243-248.
8. Pfirrmann C, Metzdorf A, Zanetti M, Hodler J, Boos N. Magnetic resonance classification of lumbar intervertebral disc degeneration. *Spine*. 2001;26:1873-1878.
9. Norcross JP, Lester GE, Weinhold P, Dahners LE. An in vivo model of degenerative disc disease. *J Orthop Res*. 2010;21:183-188.
10. Maclean JJ, Lee CR, Grad S, Ito K, Alini M, Iatridis JC. Effects of immobilization and dynamic compression on intervertebral disc cell gene expression in vivo. *Spine*. 2003;28:973-981.
11. Adams MA, Roughley PJ. What is intervertebral disc degeneration, and what causes it? *Spine*. 2006;31:2151-2161.
12. Chan S, Ferguson SJ, Gantenbein-Ritter B. The effects of dynamic loading on the intervertebral disc. *Eur Spine J*. 2011;20:1813.
13. Setton LA, Chen J. Cell mechanics and mechanobiology in the intervertebral disc. *Spine*. 2004;29:2710-2723.
14. Yurube T, Hirata H, Kakutani K, et al. Notochordal cell disappearance and modes of apoptotic cell death in a rat tail static compression-induced disc degeneration model. *Arthritis Res Ther*. 2014;16:R31.
15. Ching CTS, Chow DHK, Yao FYD, Holmes AD. The effect of cyclic compression on the mechanical properties of the inter-vertebral disc: an in vivo study in a rat tail model. *Clin Biomech*. 2003;18:182-189.
16. Court C, Colliou OK, Chin JR, Liebenberg E, Lotz JC. The effect of static in vivo bending on the murine intervertebral disc. *Spine J*. 2001;1:239-245.
17. Lotz J. Compression-induced degeneration of the intervertebral disc: an in vivo mouse model and finite-element study. *Spine*. 1998;23.

How to cite this article: Ji Y, Zhu P, Zhang L, Yang H. A novel rat tail disc degeneration model induced by static bending and compression. *Anim Models Exp Med*. 2021;4:261–267. https://doi.org/10.1002/ame2.12178